

Electronic structure and bonding at SiC/AlN and SiC/BP interfaces

Walter R. L. Lambrecht and Benjamin Segall

Department of Physics, Case Western Reserve University, Cleveland, Ohio 44106

(Received 19 June 1990)

The (110) interfaces SiC/AlN and SiC/BP between the cubic (sphalerite) crystals of these semiconductors are studied within the local-density-functional framework using the linear muffin-tin orbital method and the supercell approach. The preferred bonding configurations are found to be Si—N and C—Al for the former and Si—B and C—P for the latter. Both correspond to cation-anion bonding when the anomalous ion character of BP is taken into account. The latter is independently confirmed by our calculations. The interface energies are calculated as the limits of half the superlattice energies of formation and are found to be 0.45 and 0.50 eV for SiC/AlN and SiC/BP, respectively. Combined with a simple bond-breaking model for the surface energies they are used to estimate the adhesion energies, which are shown to be comparable in magnitude to the surface energies of the individual materials. The energy of formation of the 1 + 1 superlattices, which is effectively a 50% mixed compound, is calculated and used to make a crude estimate of the energy of formation and the maximum miscibility-gap temperature of the solid solutions. The band structures of the bulk compounds are presented, including an approximate correction of the band gap. The band alignment is found to be of type I for SiC/AlN and of type II for SiC/BP with the higher valence-band maximum in BP. Strain effects in the case of SiC/BP are briefly discussed. The interface electronic structures including interface states and resonances are analyzed in terms of the local densities of states.

I. INTRODUCTION

Recently, there has been increasing interest in wide-band-gap semiconductors.¹ There are several motivations for this interest. Wide band gaps are required for high-temperature applications and for electro-optical applications in the short-wavelength range of the visible spectrum and the near uv. The II-VI compounds, such as the selenides and tellurides of zinc and cadmium, which have been the principal candidates for such applications in the past, have notable doping problems.² Consequently, a number of alternative materials are being considered: SiC, diamond, *c*-BN, GaN, etc. It is too early to predict whether the electrical properties of these materials will prove to be more tractable than those of the II-VI compounds. Whether or not that is the case, these wide-band-gap semiconductors form an interesting class of materials in themselves, and that clearly justifies their study.

On the basis of Harrison's³ simple picture of the bonding in tetrahedral semiconductors, one can either increase the *ionicity* or the *covalent* interaction between the atoms to widen the band gap. Clearly the former alternative is pursued in the II-VI compounds. Since the covalent interaction is strong for early elements in the Periodic Table, in particular, for the elements of the second row, such as B, C, and N, the latter alternative can be used for semiconductors involving these elements. One way to understand this is to note that the $2p$ orbitals are quite localized because of the lack of lower p -type core

orbitals. These elements thus have small atomic radii and strong covalent interactions. As a result, among the group-IV elements, C in the diamond structure has the strongest covalent interaction and the widest band gap. The compound semiconductor most closely related to diamond is *c*-BN. We have previously studied the interface between these two materials.⁴ The next series of closely related materials involves elements from the second and the third row: SiC, BP, and AlN. These are the subject of this paper. The other materials of interest within this series of nitrides and borides are GaN, InN, and BAs.

Heterostructures form an interesting alternative to the traditional *p-n* junction technology and could be useful even in the event that some of the materials of interest cannot be doped both *p* and *n* type. The doping possibilities of the nitrides mentioned above have recently been analyzed theoretically by Jenkins and Dow.⁵ BP can be doped both *p* and *n* type.⁶ Epitaxial growth of (wurtzite) AlN on 6H-SiC was reported by Knippenberg and Verspui⁷ while Rutz and Cuomo⁸ reported growth of SiC on AlN substrates. Recently, Paisley *et al.*⁹ reported the successful growth of GaN and GaN/AlN layered structures on SiC. Although the usual form of AlN, GaN and InN is the (hexagonal) wurtzite structure, it proved possible to grow both hexagonal and cubic GaN on a SiC substrate depending on the crystal structure and surface of the substrate, the growth temperature, etc. Similar results are expected for AlN (and InN) but have yet to be realized in practice.

Since the wide band gaps in these materials are due to the strong covalent interaction, all these materials are also very interesting for their mechanical properties. Their strong bonding is manifested in their high cohesive energies, elastic constants, and their hardnesses. This makes them useful for reinforcement in metal-ceramic and ceramic-ceramic composites. Again, the interfacial properties are likely to play a crucial role in connection with these applications.

Finally, the strong covalent tetrahedral bonding results in a high phonon-mediated thermal conductivity in this class of materials.¹⁰ Since they combine this property with a wide band gap and thus a low dielectric constant typical of good insulators, they are very attractive for heat sink applications, e.g., as substrates or packaging material for semiconductor devices. AlN, in particular, has recently been extensively investigated from this point of view.¹¹ Because of its close lattice match to SiC, AlN substrates should be an attractive substrate possibility for SiC.

The above considerations provide strong motivation to study interfaces between the above-mentioned semiconductors. In this study, AlN and BP were chosen because of their (relatively) close lattice match to SiC. The present study is limited to the constituents with cubic (zinc-blende or sphalerite) crystal structure. Since the nearest-neighbor coordinations in the wurtzite and the sphalerite structures are the same, the general conclusions concerning the bonding arrived at in this work should also be valid to interfaces involving the wurtzite structure.

We focus on the (110) interface for several reasons, to be explained in detail in Sec. II. Briefly, the main reason for this choice is that the heterojunctions considered here are nonisovalent. This implies that the abrupt *polar* interfaces would be metallic and have a higher energy. Interdiffusion leading to a compensation of III-IV and IV-V bonds would prevent the formation of a metallic interface and is expected to occur.^{12,13} This complicates the study of the polar interfaces, e.g., (001) and (111), but is also expected to make them more similar (at least qualitatively) to the (110) interface, which is *nonpolar*.

The anomalously deep-lying $2s$ and $2p$ levels have a marked effect on the ionicity of these semiconductors. Since, in the case of BP, the anomalously deep valence levels belong to the group-III atom, the ionicity of this compound is strongly reduced compared to other III-V semiconductors. For AlN, on the other hand, the deep valence levels are those of the group-V atom (N in this case) and that appreciably enhances the ionicity.³ It is thus of special interest from a theoretical point of view to compare the behavior of BP and AlN in their interfaces with SiC. As we will show, the ion character in BP is actually reversed, B playing the role of anion. Independently, Wentzcovitch *et al.*¹⁴ came to the same conclusion and provided additional evidence for the inverted ion character on the basis of the behavior of BP (and BAs) under high pressure. In the present problem of in-

terfacial bonding, it results in a seemingly unexpected bonding configuration, when compared to the SiC/AlN interface.

In this paper, we report the results of first-principles electronic structure calculations for these semiconductors and their interfaces. We will be concerned with both the energetics, i.e., the energies of formation of the interfaces and the minimum energy bonding configurations, and the electronic properties, such as the band offsets and the local densities of states near the interface. The interface energies are used to estimate the adhesion energies. This requires as additional information the surface energies. The latter are estimated rather crudely from the bulk cohesive energies and a simple bond-breaking model. In spite of the crudeness of this approach, it allows us to show that there is almost an order of magnitude difference between the surface and the interface energies. As a consequence, the interface energies have only a small effect on the adhesion energies for the two heterojunctions studied here.

The supercell approach is used for modeling the interfaces. Our calculations thus also provide information on small-period superlattices and to a limited extent on the possibilities of forming intermediate compounds and solid solutions. Solid solutions of SiC and AlN have been reported and a tentative phase diagram was constructed by Zangvil and Ruh.¹⁵ The optical absorption and photoluminescence of SiC-AlN solid solutions have recently been studied by Nurmagomedov *et al.*¹⁶

A preliminary account of some aspects of this work has previously been given in conference proceedings.¹⁷⁻¹⁹ The band offset of SiC/AlN was included in a general paper on the theory of band offsets.²⁰

Since we initiated this work, one other study of the SiC/AlN interface bonding has appeared in the literature. Nath and Anderson²¹ used a semiempirical approach to study the bonding at various polar and nonpolar interfaces between wurtzite AlN and cubic and wurtzite SiC. Since they did not present values for the interface energy as we calculate it here and did not consider the question of band alignment, a straightforward comparison to their work is difficult. Also, they assumed all the interfaces (the polar as well as the nonpolar) to be abrupt. In Sec. II we will argue that this is an unrealistic assumption for the polar interfaces because of the expected interdiffusion.

The paper is organized as follows. In Sec. II we discuss our choice of the (110) interface and the expected interdiffusion for polar interfaces. Section III presents some details on the computational method. Section IV presents our results for the energetics of the interfaces. Section V discusses the band structure of the individual materials, the band offsets, and the interface local densities of states. Section VI summarizes our conclusions.

II. CHOICE OF INTERFACE

For nonisovalent heterojunctions, such as the SiC/AlN and SiC/BP interfaces considered here, abrupt polar in-

interfaces are expected to be metallic, because of the occurrence of undersaturated or oversaturated bonds. Interdiffusion, at least at the level of one and possibly several atomic layers, is expected as was first pointed out by Harrison *et al.*¹² This leads to the elimination of the electrostatic fields which would otherwise occur for abrupt polar interfaces. The expected magnitude of the latter is strong enough to give rise to a potential difference of the order of the band gap within a few atomic layers. This situation would induce important accumulation of mobile charge carriers due to the resulting short circuiting. That these effects have not been observed for any semiconductors provides indirect evidence that a compensating interdiffusion must take place. Direct experimental evidence for interdiffusion at the atomic level in semiconductor heterojunctions was recently provided by Ourmazd *et al.*²² These authors showed that interdiffusion even exists for isovalent cases such as $\text{Al}_x\text{Ga}_{1-x}\text{As}/\text{GaAs}$ and depends strongly on the growth temperature. Martin¹³ showed that compensation of the undersaturated and oversaturated bonds is energetically favorable.

Compensation is achieved automatically without the need for interdiffusion at the nonpolar (110) interface. Since the more complex reconstructed polar interfaces would be characterized by the occurrence of the same types of compensated bonds, the effective average bonding is not expected to be drastically different from that at the (110) interface. This, of course, does not exclude the possibility that small energy differences may exist for different interfaces.

In previous work, we have analyzed the effects of the interface stoichiometry on the band offsets for nonisovalent heterojunctions by means of the "interface-bond-polarity model,"²³ which we had developed. The main result of that work is that important differences between the (110) and the (001) band offsets can exist for specific chemical reconstruction patterns, which, for example, are characterized by purely cation or purely anion interdiffusion. These can be described simply in terms of the difference in valency, the lattice parameters, and the average dielectric constant. If, on the other hand, cation and anion interdiffusion occur in equal amounts, the difference between the (110) and (001) offsets vanishes (in this model). Although more work is required to study which of the interface chemical reconstructions is most stable, this average situation seems to be the most plausible in view of the fairly elevated growth temperatures. A certain degree of disorder in the actual intermixing without preference for cation or anion diffusion was suggested by Martin's analysis¹³ of the problem using an Ising spin model.

In summary, although a detailed analysis of other interfaces would be interesting, a study of the (110) interface presumably represents the essential features of the interface electronic structure and energetics when the averaging effects of the expected interdiffusion on polar interfaces are taken into account.

III. METHOD OF CALCULATION

The approach followed in this work is based on the Hohenberg-Kohn-Sham density-functional method in the local-density approximation (LDA).²⁴ We use the von Barth-Hedin parametrization²⁵ of the exchange-correlation potential. Andersen's linear muffin-tin orbital (LMTO) method²⁶ is used in the atomic-sphere approximation (ASA). As usual for the open sphalerite structure, so-called empty spheres²⁷ are introduced at the tetrahedral interstitial sites in order to provide an adequate description of the charge density and potential in those regions. Slightly overlapping space filling and equally sized Wigner-Seitz spheres [of radius $s = (3/\pi)^{1/3}a/4$ with a the cubic lattice constant] are used on all sites. The ASA with interstitial empty spheres has successfully been used in many previous calculations on semiconductors and interfaces. Bachelet and Christensen²⁸ have explicitly shown for GaAs that the ASA provides results in very good agreement with first-principles pseudopotential calculations which do not make spherical shape approximations to the potential. Since the present calculations are essentially restricted to bulklike geometries, the same accuracy can be expected here for the supercell calculations. Christensen's²⁹ calculations of the energy of formation of $(\text{GaAs})_n(\text{AlAs})_n$ superlattices show that even for small energy differences (of the order of 0.01 eV) the ASA results are in agreement with those from calculations without shape approximation. Finally, we note that Andersen *et al.*³⁰ have recently explicitly shown that the overlapping ASA potential is very close to the general self-consistent LDA potential without shape approximation. The problems with the ASA seem to result rather from the use of the spherical approximation for the charge density in the final total-energy expression than from the spherical approximation to the potential. This would indicate that even in the particular cases where problems are known to occur for the energetics in the ASA [e.g., the instability of the diamond structure to a $\text{TO}(\Gamma)$ phonon distortion, which involves a very small energy difference of the order of 0.01 eV and substantial changes in the overlap of the spheres], the electronic structure may still be reasonably well described. In fact, the errors in the corresponding ASA deformation potentials are typically about 30%.³¹ These are not unphysical as are the total energies for the same distortions. The above indicates that we have to exercise considerable caution when considering distortions of the ideal sphalerite structure. An example that we encounter in this paper occurs in a calculation for orthorhombically strained BP on SiC (110). We find that loss of accuracy due to the ASA in deformation potentials and energetics are less severe for distortions along the (001) than along the (111) direction. For the (110) distortions the situation should be intermediate between those for the (001) and (111) directions. Discussion of these results will appear elsewhere.

To study the interfaces we follow the common practice of using a supercell approach. Since the (110) plane is a mirror plane of the sphalerite structure, a stoichiometric supercell can be constructed with two equivalent interfaces. The energy of formation of the interface (*interface energy* for short) is thus half the energy of formation of the superlattice A_nB_n in the limit of large n . In practice, the energy converges very rapidly, and as we will show, a good approximate value is obtained for $n = 3$. The energy of formation of the superlattices is obtained simply by subtracting from the total energy of the A_nB_n superlattice that of the equivalent number of atoms in the corresponding bulk materials,

$$\Delta E_f(A_nB_n) = E(A_nB_n) - \frac{1}{2}[E(A_{2n}) + E(B_{2n})]. \quad (1)$$

The two bulk energies are calculated using a supercell of the same size and in exactly the same manner, in particular, with the same set of \mathbf{k} points. This procedure reduces systematic errors, resulting from such effects as different cutoffs in the numerical computations. In what follows, we will usually normalize the energy of formation of the superlattice to an interface unit-cell area. That is, we will use half of Eq. (1) so that its limit for large n approaches the interface energy per unit-cell area.

As we will show, cubic AlN is almost perfectly lattice matched to cubic SiC. Although BP has a 4% larger lattice constant than SiC, we have considered the interfaces for BP hydrostatically compressed to the lattice constant of SiC. For BP, grown epitaxially on SiC, one actually expects that its in-plane lattice constant would be compressed to match that of the substrate. The BP film would be distorted in the perpendicular direction according to the Poisson ratio. The strain effects are not expected to appreciably modify our general conclusions about the bonding. They may, however, have an effect

of the order of 0.1 eV on the band offset. Further work on these strain effects is required since it is expected to depend rather strongly on the interface orientation.

IV. ENERGETICS

A. Bulk properties

Table I presents the equilibrium lattice constants, bulk moduli, and cohesive energies, along with the available experimental data. The calculations were performed nonrelativistically which should be entirely adequate for these light elements. The total energy as a function of lattice constant over a range of about 5% in compression and expansion around the equilibrium was fitted to the universal energy relation of Vinet *et al.*³² in order to extract the desired properties. The agreement with the experimental data is satisfactory, considering the experimental uncertainties for these materials and the usual overestimate of the cohesive energies owing to the LDA.

B. Interface energy

In Table II the energies of formation of the superlattices $(\text{SiC})_n(\text{AlN})_n$ and $(\text{SiC})_n(\text{BP})_n$ are given as a function of the size n . They are normalized per interface unit-cell area. The interface bonding configurations considered are the Si—N,C—Al bonding and the Si—B,C—P bonding. These will be shown to be the stable configuration in Sec. IV D.

For SiC/AlN we can see that the energy rapidly approaches a constant value: the interface energy of an isolated interface. Only the 1 + 1 superlattice has a slightly different energy. It is found to have a slightly lower energy per interface. The same result was also obtained for

TABLE I. Equilibrium lattice constant, bulk modulus, and its pressure derivative and cohesive energy for cubic SiC, AlN, and BP.

		a (Å)	B (GPa)	B'	E_{coh}^a (eV/pair)
SiC	(theory)	4.32	233	3.8	14.06
	(expt.) ^b	4.3596	224		12.68
AlN	(theory)	4.33	215	3.9	12.74
	(expt.) ^c	4.37	206		11.54
BP	(theory)	4.51	172	3.7	11.45
	(expt.) ^d	4.538	173		10.24

^aIncludes spin-polarization correction for atoms as follows: Si (0.76 eV), C (1.27 eV), Al (0.19 eV), N (3.15 eV), B (0.28 eV), and P (1.77 eV) and zero-point motion energy ($9k\Theta_D/4$) as follows: SiC (0.21 eV), AlN (0.18 eV), and BP (0.19 eV), where k is Boltzmann's constant and Θ_D the Debye temperature.

^b*Landolt-Börnstein Tables*, Ref. 64, for lattice constants and bulk moduli and Wagman *et al.*, Ref. 68, for cohesive energies.

^cThe lattice constant corresponds to the cubic structure with the equivalent volume per atom as the observed wurtzite structure. Bulk modulus from P. Boch, J. C. Glandus, J. Jarrige, and J. P. Lecompte, *Ceramics International* **8**, 34 (1982).

^dBulk modulus from elastic constants measured by Wettling and Windscheif, Ref. 69.

TABLE II. Energy of formation of superlattices normalized per interface unit-cell area.

	ΔE_f (eV)
(SiC) ₁ (AlN) ₁	0.40
(SiC) ₃ (AlN) ₃	0.45
(SiC) ₅ (AlN) ₅	0.45
(SiC) ₁ (BP) ₁	0.40
(SiC) ₅ (BP) ₅	0.50

diamond/c-BN.⁴ Of course, if we normalize the energy of formation per atom, the energy of formation is found to be monotonically decreasing since the cells contain more and more bulk material.

Figure 1 shows that the nearest-neighbor coordination in the 1 + 1 cell is different from the larger cells. However, from $n = 2$ on, the interface atoms already have the same nearest-neighbor configuration as near an isolated interface. For $n = 2$ all the layers are interfacelike in this sense, while in the $n = 3$ case considered here, there is a distinguishable interfacelike and bulklike layer. In other words, the 1 + 1 cell is not really meaningful as a representation of the interface structure. It represents a truly mixed compound. The rapid convergence of the energy of formation of the superlattice indicates the dominance of the nearest-neighbor interactions.

C. Adhesion energy

A quantitative measure of the interfacial bond strength is provided by the *adhesion energy* W_a , given by

$$2W_a(A/B) = \gamma_s(A) + \gamma_s(B) - \gamma_i(A/B), \quad (2)$$

in terms of the surface energies γ_s of the pure materials and the interface energy γ_i discussed in Sec. IV B. The factor of 2 in this equation normalizes the adhesion energy per surface unit-cell area of the two separated surfaces. Thus, for a pure solid, it equals the surface energy.

The calculation of surface energies is possible using the same supercell technique as here used for the interfaces by introducing a number of empty layers representing the vacuum. However, the perturbation of the local electronic structure from the bulk is much stronger near a

free surface than for an solid-solid interface. The laterally averaged electrostatic potential varies rapidly from its internal value in the solid to its value outside in the vacuum. Over about one interplanar distance it can typically change by a few eV. This invalidates the use of the ASA,²⁶ in particular, the use of a spherical charge density on the surface atom and on the first layer of empty spheres which would represent the vacuum. In fact, the dipole character of these charge densities is expected to be strong in the direction perpendicular to the surface. Furthermore, the free surfaces are expected to exhibit important atomic relaxations. A universal type of atomic relaxation, involving an outward movement of the anion and a relatively inward movement of the cation has been proposed to exist for III-V and II-VI compounds by Duke and Wang.³³ The relaxation is universal in the sense that the bond angles are approximately the same for many systems.

We have attempted calculations for the ideal surface cleavage energy within the ASA for SiC, AlN, and GaAs and found that the surface energies were overestimated by a factor of 4 or more and are thus meaningless. In spite of this the calculations captured the essential features of the surface local densities related to the dangling bonds expected on such surfaces and did not give unreasonable values for the work function.¹⁷ Calculations of the surface energies that take into account the essential nonspherical contributions to the energy are in progress.

For lack of a reliable calculation of the surface energies at this stage, we here resort to a very simple estimate in terms of a bond-breaking model. As a unit-cell area of the (110) surface is essentially formed by breaking a single nearest-neighbor bond, the surface energy should be the energy of a single bond. Within the same approximation, the latter corresponds to one-quarter of the cohesive energy per atom since each atom has four bonds. From the cohesive energies in Table I, the bond energies are 3.5 eV, 3.2 eV, and 2.9 eV for SiC, AlN, and BP, respectively. The adhesion energies are then found to be: 3.1 eV for SiC/AlN and 3.0 eV for SiC/BP. It is seen that the interfacial energy makes only a small contribution (less than 10%) to the total adhesion energy.

As an indication of the accuracy of the bond-breaking model, we consider the case of GaAs, where a reliable calculation of the (110) surface energy is available. The

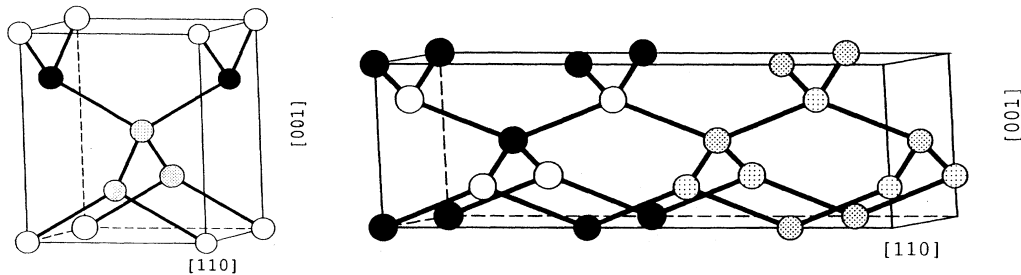


FIG. 1. Bonding configurations in a 1 + 1 and 3 + 3 supercell of the sphalerite structure.

surface energy of the relaxed GaAs (110) surface was calculated by Qian *et al.*³⁴ to be 1.22 eV/surface-unit-cell-area including a 0.35 eV contribution from atomic relaxation. The ideal surface energy is thus 1.57 eV. The experimental cohesive energy of GaAs is 6.34 eV per atom. Thus the bond-breaking estimate would give 1.7 eV, which is only a 10% overestimate. The surface relaxation contribution is found to be about 20%. Making the plausible assumption that similar corrections will apply to the present materials, we may thus expect that the surface and adhesion energies given above are $\sim 30\%$ overestimates. With the inclusion of this correction, we would find 2.5 eV, 2.2 eV, 2.0 eV as our final estimates for the surface energies of SiC, AlN, BP, respectively. This, in turn leads to 2.1 eV and 2.0 eV for the SiC/AlN and SiC/BP adhesive energies. Our justification for this *ad hoc* rescaling of the energies is twofold: first the universal nature of the surface relaxation³³ and second the existence of a universal bond energy-distance relationship in the bonding of various materials in various geometries³⁵ which indicates that surface energies should indeed scale as cohesive energies. Nevertheless, the above remains, of course, a rather crude estimate instead of an actual calculation. The uncertainty is at least several tenths of an eV. We note that these surface or adhesion energies are of the order of 0.15 eV/Å² or 2.4 J/m². This is large compared to typical adhesion energies in metals or metal/ceramic interfaces and reflects the strong bonding in these materials.

D. Bonding configuration

Table III compares the energies of formation obtained in Sec. IV B to the ones obtained with the other possible interface bonding configurations. Clearly, the energy differences are sufficiently large to suggest that the alternative bonding configurations would never occur. Inserting these interface energies in Eq. (2) yields a negative adhesion energy for SiC/AlN and a small but positive value for SiC/BP. We note, however, that relaxation of the bond lengths lowers the interface energy to a degree dependent on the magnitude of the relaxation. This could be significant in the case of the Si—Al bonds which are here in a very compressed state. Previous calculations on SiC inversion domain boundaries³⁶ where Si—Si bonds occur — a situation quite similar to the present Si—Al,C—N configuration — have shown that relaxation

TABLE III. Interface energy per interface unit-cell area as a function of bonding configuration.

Interface	Bonding	γ_i (eV)
SiC/AlN	Si—N,C—Al	0.45
	Si—Al,C—N	8.10
SiC/BP	Si—B,C—P	0.50
	Si—P,C—B	3.57

of those bonds lowers their energy by as much as 50%. But even with such a decrease in the present problem, the energy would still be of the order of a few eV rather than a few tenths of eV. The present calculations for the unrelaxed geometries thus indicate quite convincingly that these bonding configurations are energetically unfavorable.

Furthermore, for the case of SiC/AlN, the above result is readily understandable. For electrostatic reasons, it is obvious that the cations prefer to bond to the anions. Since, in SiC, the lower valence levels are associated with the carbon atom, it plays the role of anion. In AlN, the group-V element N is clearly the anion. The fact noted earlier that this second row element has particularly deep valence levels only enhances its anionic character. The result for SiC/BP is, at first sight, surprising because P is the group-V element which generally exhibits anionic character. Nevertheless, it can be explained in the same way by assuming that B plays the role of anion and P that of cation.

In fact, a look at the net charge per sphere, including the empty spheres in Table IV shows that the P sphere is positive and the B sphere is negative. The reason for this anomalous ion character for a III-V compound can again be traced back to the deep-lying valence levels of the B. As a result of these deep valence states B attracts a large amount of electronic charge.

A word of caution with respect to this conclusion of an inverted ion character is in order. The charge ascribed to an atom in the solid is somewhat arbitrary as it depends crucially on the sphere size chosen for each atom. Clearly, if one would choose a small sphere for B in accordance to its conventional atomic radius, one would find fewer electrons associated to B. One would thus possibly ascribe cationic character to B and anionic character to P. From the point of view of the ASA-LMTO calculations, equal sphere sizes are preferable because they minimize the errors due to the overlapping of the spheres. Within a reasonable range, of course, the total-energy and band-structure results are independent of the sphere size, when the so-called combined correction term²⁶ is included.

Another way of associating charge to a specific atom is to assign the charge to certain atomic orbitals. For semiconductors, a commonly used and physically transparent basis set consists of the sp^3 -hybrid orbitals.³ Converting the present ASA results to an effective sp^3 model,²³ we find that the B sp^3 level lies above the corresponding P level. This might seem to indicate that the P attracts more electronic charge and thus would be the anion. However, the net charge per site Q also involves the valency Z and within the bond-orbital model³ is given by

$$Q = Z - 4 \pm 4\alpha_P. \quad (3)$$

In Eq. (3) α_P is the bond polarity, which characterizes the ionicity.³⁸ The plus sign is taken for the atom with the higher valence level. The LMTO polarities obtained

TABLE IV. Bulk charges (in units of $|e|$) per atomic or interstitial sphere.

	SiC		AlN		BP
Si	2.022	Al	1.864	B	-0.087
C	-0.347	N	-0.458	P	1.869
E_1^a	-0.871	E_1	-0.792	E_1	-0.940
E_2	-0.804	E_2	-0.654	E_2	-0.842

^a E_1 has C, N, or P atoms as nearest neighbors, and E_2 has Si, Al, or B atoms as nearest neighbors.

for SiC, AlN, and BP are, respectively: 0.4725, 0.8077, and 0.0181. This clearly shows the large ionicity of AlN and the very low ionicity of BP. As a result of this low ionicity of BP the net charge on the B site deduced from Eq. (3) is negative, in agreement with our direct band-structure result. The corresponding Harrison polarities deduced from atomic term values are 0.26, 0.58, and 0.20, respectively. Although the effect is less pronounced in this case, his model still predicts a negative charge for B in BP.³

For the present purpose of studying the energetics of the interface and trying to understand it in terms of electrostatic effects, the equal sphere size distribution of the charge seems to be the least biased. Of course, the charge distribution throughout space is the only real, and, in principle, observable quantity, which through density-functional theory determines the total energy. The ASA approach of lumping the charge into spheres and spherically averaging it over each sphere so that the intersphere interaction reduces to point charges is convenient but certainly not unique. The relative role of intersphere and intrasphere contributions will, of course, change as one changes the sphere radii. Here, we interpret the high energy of the Si—P,C—B configuration as being a result of the unfavorable intersphere interaction between spheres with charges of the same sign. However, with another choice of spheres, the same electrostatic repulsion could appear in the intrasphere terms. Whichever way one wants to look at this problem, the physics clearly is that the deep levels of B draw a large amount of electronic charge near to it and this negative charge distribution prefers to sit closer to the more positive Si sites than to the more negative C sites on the SiC side.

We note that there are some independent indications of the inverted ion character of BP. Wentzcovitch *et al.*¹⁴ showed that the high-pressure behavior of BP is anomalous and corresponds to an inverted ion character from what is observed for other III-V compounds. Furthermore, B impurities in SiC are known to be substitutional on the C site, i.e., preferring a Si—B bonding.^{38,39} The latter may possibly also be related to the size effect, B being more similar in size to C than to Si.

Finally, we note that for the nonpolar interfaces between wurtzite SiC and AlN, Nath and Anderson²¹ also came to the conclusion that Si prefers to bond to N and C to Al. Nevertheless, there are important differences between their treatment of this problem and ours. We find the high energy of formation for the oppo-

site configuration to be due primarily to the unfavorable electrostatic interactions. Their treatment does not include long-range electrostatic terms and thus misses this effect. Instead, they introduce an additional charge-transfer-stabilization term in the calculation for the Si—N,C—Al configuration which favors that atomic arrangement, but they did not include it for the other configuration. Moreover, within a linear-combination-of-atomic-orbitals (LCAO) approach, the ionic contribution to the bonding is already contained through the differences in the atomic term values.⁴⁰ Adding an extra charge-transfer-stabilization term proportional to the difference in atomic term values, as they do, is thus including the same effect twice, although in different ways. This is an incorrect procedure. Leaving out this additional term from their calculations, one would still obtain the Si—N,C—Al bonding to be preferred although less strongly so. As pointed out above, their treatment misses the destabilizing electrostatic effect for the Si—Al,C—N configuration.

E. Solid solutions

The positive energies of formation of the superlattices indicate their instability towards disproportionation into the individual semiconductors. For the present discussion, it is convenient to normalize the energy of formation per atom. For the 1 + 1 superlattice, which effectively is a 50% composition mixed compound, we thus obtain 0.20 eV/atom for SiCAlN and SiCBP. This is fairly large compared to that of semiconductor superlattices such as (AlAs)₁(GaAs)₁ for which this energy is of the order of 10 meV.^{29,41,42} The disordered solid solution of 50% composition would have a somewhat lower energy than the ordered solid of the same composition because of the occurrence of local environments with higher or lower concentrations of a given component than the average. These local environments are closer to the dilute limit and thus are expected to cost less energy to form. At a finite temperature, the free energy is further reduced by the entropy terms and for a sufficiently elevated temperature the mixed state becomes thermodynamically stable relative to the phase-separated state. It is the purpose of this section to estimate the maximum *miscibility-gap temperature* at which this happens. A first-principles calculation of the full temperature-composition phase diagram of a four-component system such as SiCAlN is outside the

scope of this paper. Analogous calculations have only recently become the object of intensive study for simpler pseudobinary systems involving the more traditional semiconductors.^{42,43} Here, we will only sketch briefly how such a calculation would proceed and make a crude estimate.

We assume that the energy of formation of the disordered solid solution can be written as the sum of the energies for a relatively small number of representative local configurations or clusters. For semiconductors, the usual choice for the latter are the various tetrahedral nearest-neighbor coordinations of each cation or anion. The situation is somewhat more complicated here than for the pseudobinary systems with a common anion that have been studied so far.^{42,43} However, we will assume that there is no *antisite* disorder: i.e., the cations stay on one sublattice and the anions on the other. In fact, this assumption is also made in most treatments of the pseudobinaries. We thus consider a combination of two binary alloy problems. Our justification for this is the large energy cost in forming cation-cation or anion-anion bonds as evidenced in our study of the corresponding interface bonding configurations. Furthermore, we will assume that the clusters are not completely independent but must occur in combinations which preserve *local stoichiometry*. If, for example, a Si is surrounded by three C and one N, then we assume that each N must also be surrounded by one Al and three Si. For the same reason, we exclude local environments such as a Si surrounded by four N. As in the Connolly-Williams approach,⁴⁴ we determine the energies of these clusters (or here cluster combinations) by performing total-energy calculations for *ordered* structures, in which precisely these clusters (or cluster combinations) occur exclusively. The 1 + 1 superlattice considered above represents the bonding configuration in which each Si is surrounded by two C and two N, each C by two Al and two Si, etc. Similarly, it is straightforward to construct ordered structures corresponding to the compositions (SiC)₁(AlN)₃, in which each Si is surrounded by one C and three N, etc. and correspondingly for (SiC)₃(AlN)₁. For simplicity, however, we will here assume that the energies of the latter can be obtained by interpolation between the value for the (SiC)₁(AlN)₁ and the pure semiconductors (with zero energy of formation by definition). Assuming a parabolic dependence on the concentration $x = n/4$, we obtain

$$\Delta E_n = 4\Delta E_2 \frac{n}{4} \left(1 - \frac{n}{4}\right) \quad \text{for } n = 0, \dots, 4, \quad (4)$$

where ΔE_2 corresponds to the 1 + 1 superlattice of 50% composition calculated above to be 0.20 eV/atom. For the cluster combinations corresponding to 25% and 75% composition, we thus obtain $\Delta E_1 = \Delta E_3 = \frac{3}{4}\Delta E_2 = 0.15$ eV.

For the disordered solid solution of composition x , we assume that the various cluster combinations occur with a *random* probability. This leads to an average energy of formation

$$\Delta E_d(x) = \sum_{n=1}^3 \binom{4}{n} x^n (1-x)^{4-n} \Delta E_n. \quad (5)$$

We note that in reality the probability distribution of clusters is not random but weighted by their respective energy and should be determined by minimizing the free energy including the entropy terms, as is done in the cluster variation method^{45,46} or the quasichemical approximation.⁴³ For the present crude estimate, however, this approximation should suffice. Consistent with the above neglect of partial ordering, we take the entropy to be that of random mixing which is given by its classical expression (normalized per atom)

$$\Delta S_m(x) = -k[x \ln x + (1-x) \ln(1-x)], \quad (6)$$

where k is the Boltzmann constant. The free energy at a given temperature T and composition x is thus

$$\Delta F(x, T) = \Delta E_d(x) - T\Delta S_m(x). \quad (7)$$

Because of the assumed form for $F(x)$ the relevant extremum occurs at the concentration $x = 0.5$. The miscibility-gap temperature T_s is the temperature at which this extremum becomes a minimum: i.e., $d^2 F/dx^2 \geq 0$.⁴⁷ A little algebra shows that within our specific model this occurs for

$$T_s = 3\Delta E_2/2k. \quad (8)$$

Since ΔE_2 is the central energy in the model, T_s must, of course, be proportional to $\Delta E_2/k$. The accuracy of the result is tied to the numerical factor which here is $\frac{3}{2}$. A more simplified model than the present one results if one would take $\Delta E_d(x)$ to be the mean field expression which is given in Eq. (4). A simple calculation shows that this leads to a factor of 2 in place of the $\frac{3}{2}$.⁴⁷ The reason that the present model leads to a lower value is it effectively involves a larger range of configurations. That in turn leads to a lower average energy. But the present model itself deals with a seriously restricted range of configurations and that implies that the correct factor is lower than 1.5. In fact, our use of the tetrahedral clusters, which is equivalent to using only nearest-neighbor interactions in a generalized spin model of the problem, has been found to lead to an overestimate of T_s by as much as 50% in studies of the pseudobinaries.⁴⁸ From this, it appears that a better — though admittedly still rough — estimate for T_s than Eq. (8) would be

$$T_s \approx \Delta E_2/k, \quad (9)$$

which corresponds to 2500 K for the SiC-AlN system. The uncertainty in this estimate could be of the order of ± 500 K.

Next, we consider two corrections to the above estimate. The first is the vibrational contributions to the free energy. The vibrational free energy at temperature T per atom can be estimated in a Debye model as

$$F_{ph} = 9k \frac{T^4}{\Theta_D^3} \int_0^{\Theta_D/T} \ln \left(2 \sinh \frac{x}{2} \right) x^2 dx, \quad (10)$$

where Θ_D is the Debye temperature of ~ 1000 K. For T about 2–3 times the Debye temperature the integral approximately equals -0.04 to -0.02 , respectively. The vibrational free energy per atom is then of the same order of magnitude as the energy of formation (i.e., a few 0.1 eV). However, for the contribution to the relevant free-energy difference, it is the difference of this quantity between the mixed and phase separated cases that enters. While it is difficult to estimate, it will clearly be a good deal lower than the value given by Eq. (10), possibly even by an order of magnitude. Since these effects increase the entropy we expect them to lower the transition temperature. Usually, these effects are completely neglected. Nevertheless, the present estimate shows that it is not impossible that they would lower the mixing enthalpy by ~ 0.01 eV and the miscibility gap temperature by ~ 100 K.

Secondly, we note that the the lower energy structures for AlN and thus presumably also for the SiC-AlN solid solutions are wurtzitelike. In fact, the experimental solid solutions which have so far been made have a wurtzitelike structure. For SiC, as is well known, the energy difference between cubic and hexagonal phases is very small (of the order of 0.004 eV/atom),⁴⁹ which is the basic reason for the existence of the many polytypes in SiC. Since AlN normally only occurs in the wurtzite structure, the energy difference between the hexagonal and the cubic structures is larger than for SiC. We have calculated this energy difference to be 0.13 eV/atom. Details of this calculation will be reported elsewhere.⁵⁰ The result appears to be quite reasonable in comparison with other known cases, such as Si (0.01 eV),⁵¹ C (0.03 eV),⁵¹ and BeO (0.10 eV).⁵² The contribution to the energy of formation will be smaller by about an order of magnitude, so a few 0.01 eV at most seems a reasonable estimate. This, again would have the effect of lowering the miscibility gap temperature by ~ 100 K, a small effect compared to the uncertainties.

The experimental miscibility gap constructed by Zangvil and Ruh¹⁵ is rather flat as a function of temperature over most of the concentration range and places the maximum miscibility gap temperature at ~ 2300 K. In view of the crudeness of the present estimate, the agreement is satisfactory, although it is not much better than an order-of-magnitude estimate. At least it shows that the high energies of formation that we obtained can be reconciled with the known phase diagram. Clearly, much more work will be required for sorting out the effects we have mentioned. This is outside the scope of the present study which is mainly concerned with the interfaces and only discusses the solid solutions as an interesting side topic.

Finally we remark that the low ionicity of BP might lead to some degree of antisite disorder and thus tend to complicate the situation. Our calculation of the

Si—P,C—B interface bonding configuration shows, however, that even in this case the penalty for “wrong” bonding is fairly large. Nevertheless, it is somewhat lower than for SiC/AlN and relaxation of the bond lengths might lower the energy further. Similar effects could also take place for SiCAlN although the mismatch is smaller in that case. Presumably, this would lower the maximum miscibility gap temperature of SiCBP in comparison with SiCAlN.

V. ELECTRONIC STRUCTURE

A. Bulk band structures

The bulk band structures of cubic SiC, AlN, and BP at their experimental equilibrium lattice constant are shown in Fig. 2. The reference level in these figures is the ASA-reference level, i.e., the average electrostatic potential associated to the atomic sphere point charges. The values with respect to the valence-band maximum are given in Table V for some critical points in the Brillouin zone. For BP, we give the values at the lattice constant of SiC and at the 4% larger lattice constant of BP. All three semiconductors have indirect band gaps. However, whereas for SiC and AlN (and other low atomic number III-V semiconductors), the conduction-band minimum occurs at the X point, for BP it occurs slightly away from the X point along the Δ line. This is similar to diamond or Si. It is, in fact, another signature of the very low ionicity of BP. Also note that the Γ_{15}^c level in BP lies below the Γ_1^c level in contrast to SiC and AlN. We also note that the $X_3 - X_1$ splittings are a measure of the ionicity. In particular for the conduction band, note that this splitting is very small for BP and almost a rydberg for AlN. This confirms our earlier notions about the ionicity in these compounds.

As is well known, the band gaps and more generally optical interband transition energies are underestimated in the local-density-functional theory. In the first place, there is no exact justification for identifying the Kohn-Sham eigenvalues with quasiparticle excitations except for the highest occupied eigenvalue.^{53,54} As far as the minimum band gap is concerned, the discrepancy could either be due to the local-density approximation itself, or, due to the existence of a discontinuity in the exchange-correlation potential,^{55,56} or to a combination of both. The magnitude of the discontinuity is still a matter of discussion.^{57–59} In spite of this controversy, it is well accepted that Hedin’s *GW* approach⁶⁰ can provide accurate quasiparticle energies.^{58,61,62} Unfortunately, this approach requires very complex computations. In particular so far it has been applied only to materials which can be described by fairly weak pseudopotentials. On the other hand, Bechstedt and Del Sole⁶³ have made a simplified tight-binding analysis of the *GW* approach and obtained a simple analytic expression for the correction to the LDA band gap

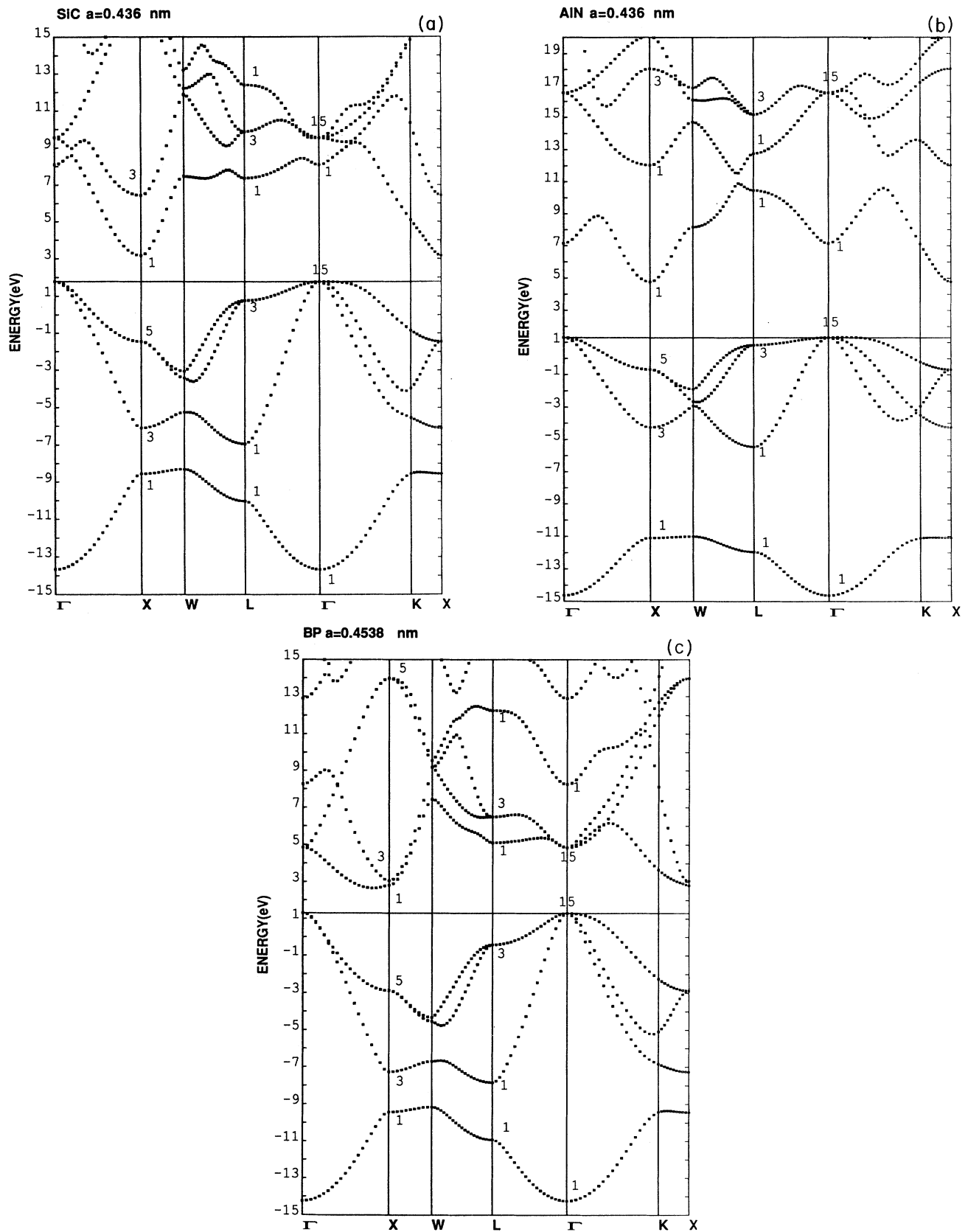


FIG. 2. Bulk band structures of sphalerite SiC, AlN, and BP.

TABLE V. Eigenvalues (in eV) for sphalerite SiC, AlN, and BP, relative to the valence-band maximum Γ_{15}^v .

	SiC	AlN	BP ($a=4.360 \text{ \AA}$)	BP ($a=4.538 \text{ \AA}$)
Γ_1^v	-15.45	-15.94	-16.69	-15.55
Γ_1^c	6.31	5.84	8.83	6.95
Γ_{15}^c	7.76	15.23	3.83	3.55
X_1^v	-10.33	-12.41	-11.11	-10.73
X_3^v	-7.88	-5.57	-9.32	-8.56
X_5^v	-3.24	-1.99	-4.65	-4.18
X_1^c	1.39	3.47	1.17	1.51
X_3^c	4.66	10.76	1.61	1.76
L_1^v	-11.81	-13.27	-12.82	-12.24
L_1^c	-8.71	-6.76	-10.16	-9.14
L_3^v	-1.01	-0.47	-1.84	-1.72
L_1^c	5.58	9.15	4.64	3.81
L_3^c	8.09	11.44	5.36	5.20
Δ_{\min}^c			1.11	1.35

$$\Delta = \frac{e^2}{\epsilon_\infty} q_{TF} / \left[1 + 7.62 q_{TF} \left(\frac{(1 - \alpha_P) r_A}{2} + \frac{(1 + \alpha_P) r_B}{2} \right) \right]. \quad (11)$$

In Eq. (11), q_{TF} is the Thomas-Fermi wave number, α_P is the polarizability (as defined by Harrison³), $r_{A(B)}$ are the cation and anion ionic radii, and ϵ_∞ is the high-frequency (electronic) dielectric constant. Within the present group of semiconductors, the correction is essentially inversely proportional to the dielectric constant. Although this simple approximation is known to have certain deficiencies — for example it corresponds to a “scissors”-type correction since it is independent of the \mathbf{k} point, which is known to be incorrect for Si (Refs. 61 and 58) — it allows for a crude estimate of the correction. The accuracy of the approximation can be estimated from the results for other semiconductors to be ~ 0.2 eV.

Table VI lists our LDA minimum band gaps, the same band gaps corrected according to Eq. (11), and the corresponding experimental values. The correction is seen to provide fair agreement with the experimental band gaps for SiC and BP. For cubic AlN, no experimental value is known. For wurtzite AlN, the LDA calculation gives a

TABLE VI. Band gaps (in eV) of sphalerite SiC, AlN, and BP.

	LDA	LDA+Eq. (11)	Expt. ^a
SiC	1.39	2.50	2.416
AlN	3.47	5.11	
BP	1.11	2.56	2.4

^a Landolt-Börnstein Tables, Ref. 64.

band gap of 5.0 eV.⁵⁰ By adding the *GW* correction we obtain 6.6 eV which is in reasonable agreement with the experimental value of 6.2 eV. Our calculation predicts that the band gap of cubic AlN is lower than that of the hexagonal structure by about 1.5 eV. For SiC the same ordering is known to occur experimentally with a band gap difference of the same order of magnitude. (The experimental band gap for SiC in the wurtzite structure — also called 2H — is 3.3 eV.⁶⁴) As one does not expect the correction to the LDA to be very structure sensitive, the difference between the band gaps for both structures should, in principle, be well described by the LDA calculation.

B. Band offsets

The valence-band offsets are calculated by means of the self-consistent-dipole theory.²⁰ In this theory, the *interface dipole* is calculated as the difference between the average electrostatic potentials produced by the point charges corresponding to the ASA spheres on the far left and right of the interface. The average is over a (110) layer, which in the bulk corresponds to a unit cell. The position of the bands with respect to this *local reference level* are determined from separate calculations for each bulk solid and together with the interface dipole lead immediately to the valence-band offset. We stress that the interface dipole has no absolute physical significance since it depends on the initial alignment of the two bulk band structures which corresponds to aligning the ASA reference levels. In our previous work, we have shown that the dipole is very insensitive to the details of the dipole profile, i.e., to the details of the charge distribution near the interface. The dipole itself can be made self-consistent without requiring self-consistency in the other degrees of freedom of the potential. Of course, one can also perform a fully self-consistent calculation, as

we have here done to obtain the total-energy results. We find the valence-band offsets to be converged with respect to the cell size for 5 + 5 supercells. In order to determine the conduction-band offsets, we include the experimental band gap where available. For cubic AlN we used our estimated band gap of 5.1 eV.

Table VII lists the calculated band offsets. No experimental determination of these quantities is available so far. The uncertainty of the valence-band offsets is estimated to be ~ 0.1 eV and slightly larger for the conduction-band offsets because of the additional uncertainties in the band gaps of AlN and BP.

We note that the AlN/SiC band alignment is of type I, i.e., the larger gap completely enclosing the smaller gap. For SiC/BP the band gaps are almost equal and the band offset is of type II, i.e., both the valence and conduction band of BP lie above the corresponding bands of SiC. This has important consequences for the carrier behavior in heterostructures. It means basically that electrons *and* holes will accumulate in the SiC regions of a SiC/AlN heterostructure. In a SiC/BP heterostructure, on the other hand, electrons would accumulate in SiC and holes in BP. Since the band offsets are all predicted to be large, these structures are promising for high-speed devices since high speed carrier injection could, in principle, be achieved across these heterojunctions.

For the purpose of light-emitting devices and solid-state lasers, it is obviously more favorable to have holes and electrons in the same region of the structure rather than in separated regions. AlN/SiC would seem to be an interesting combination for this purpose. If similar type-I behavior is obtained for hexagonal modifications of SiC, the band gap could be increased to ~ 3.3 eV in the small band-gap region of the heterostructure which determines its light-emitting frequency. The size-quantization effects in small-period superlattices would further increase the optical-transition frequency. Alloying of SiC and AlN may offer a method for additional tunability and further increase in the band gap.¹⁶ One disadvantage is that all these materials have indirect band gaps. Phonon processes are thus expected to accompany the optical transitions. We note that a (SiC)₁(AlN)₁ has a direct band gap but it is only pseudodirect since it involves a folding of the X point onto the Γ point. Thus one expects relatively weak coupling between these states and, in turn, weak optical-transition-matrix elements for the minimum band-gap transition. Only in as far as some AlN contribution becomes mixed into the wave function of this state will it differ from the

SiC X_1^c state.

The calculation presented above for SiC/BP corresponds to BP hydrostatically compressed to the SiC lattice constant. For BP layers grown epitaxially on SiC one expects the parallel lattice constant to match that of SiC while the perpendicular lattice constant in the (110) direction

$$a_{\perp} = a[1 - D_{110}(a_{\parallel}/a - 1)], \quad (12)$$

would be determined by the appropriate Poisson ratio

$$D_{110} = (c_{11} + 3c_{12} - 2c_{44})/(c_{11} + c_{12} + 2c_{44}), \quad (13)$$

where a is the cubic equilibrium lattice constant of BP and c_{11} , c_{12} , and c_{44} are its elastic constants. A direct calculation of bulk BP strained in this way along the (110) direction shows that the valence-band maximum splits into three sublevels 0.13 eV, 0.09 eV, and -0.22 eV relative to the average valence-band maximum. There is also an appreciable shift of the average valence-band maximum on an absolute scale (i.e., with respect to the ASA reference level). But, the value of the absolute shift is, in fact, meaningless. A meaningful quantity is the level position of a strained layer relative to a level in unstrained material in contact with the layer. This amounts to a band-offset problem. This problem of defining absolute deformation potentials has previously been discussed by Cardona and Christensen⁶⁵ and by Van de Walle and Martin.⁶⁶ Here, we do not make use of the deformation potentials, but instead directly calculate the band offset for the strained BP in contact with SiC.

A preliminary calculation for (SiC)₅(BP)₅ with BP strained according to Eqs. (12) and (13) yielded a valence-band offset equal to the unstrained case to within 0.1 eV, including the splitting. The interplanar distance at the interface was taken to be the average of the interplanar spacings of SiC and BP. The sphere radii in SiC and BP were kept equal to their corresponding bulk and strained layer values and are volume filling. A check of this result with full-potential (i.e., beyond ASA) calculations would be desirable. Previous calculations of uniaxial deformation potentials indicate that corrections to the ASA may be necessary.³¹ Also, relaxation of the atomic positions over and above the change in interplanar distances may be necessary in these strained cases. In our calculation, we noticed an important compensation between the change in initial band offset (i.e., the difference between the bulk valence-band maxima measured with respect to their ASA reference levels) and the corresponding interface dipole, as we anticipated on the basis of our previous work.²⁰ In any case, we expect that differences in the band offsets of the order of 0.1 eV could occur due to the different strain conditions for different interface orientations. This estimate is based on similar results for other heterojunctions with a comparable amount of strain, such as Si/Ge.⁶⁷

TABLE VII. Band offsets and band gap discontinuities (in eV).

A/B	ΔE_v^a	ΔE_c	ΔE_g
AlN/SiC	1.5	-1.2	-2.7
SiC/BP	1.2	1.1	-0.1

^a $\Delta E_{v(c,g)} = E_{v(c,g)}(B) - E_{v(c,g)}(A)$.

C. Interface electronic structure

The interface electronic structure is most conveniently discussed in terms of the layer-projected local densities of states. The layer-projected densities of states in a 3+3 superlattice of SiC/AlN for the Si—Al,C—N bonding configuration, which was found to be energetically unfavorable, are shown in Fig. 3. One may see that in this configuration interface localized states occur in the main band gap. This pushes the Fermi level up as indicated. Because of the general upward shift of the bands, this configuration can thus be seen to be unfavorable not only because of the electrostatic contribution but also in terms of the band-structure component. The localized character of the interface states can be seen from the decrease in peak height from the interface layers towards the central layers. Clearly, for a 3+3 superlattice, the central layer is not yet truly bulklike. Therefore, we show the results for a 5+5 superlattice for the favorable bonding configuration (Si—N,C—Al) in Fig. 4. No states occur in the main band gap, although there are interface states in the lower band gap, which basically separates *s*-like states from *p*-like states. Just above the valence band of AlN but below the valence-band maximum of

SiC, there are also some states localized on the AlN side. Since these states are resonant with the band continuum of SiC they are called interface resonances. These states near the valence-band maximum play an important role in establishing the charge transfer and thus the interface dipole and band offset at the heterojunction.

For SiC/BP, the layer densities of states are shown in Fig. 5 for the Si-P and C-B (unfavorable) configuration, and in Fig. 6 for the Si-B, C-P (favorable) configuration, both obtained from a 5+5 superlattice. No interface localized states occur in the semiconducting band gap in either case. In the favorable bonding case, interface states occur in the lower band gap. No obvious trend in the shift of the one-electron eigenvalues can be detected in these figures.

One may notice, that, in general, the third layer away from the interface is already fairly bulklike in character, although the interface features have not completely disappeared.

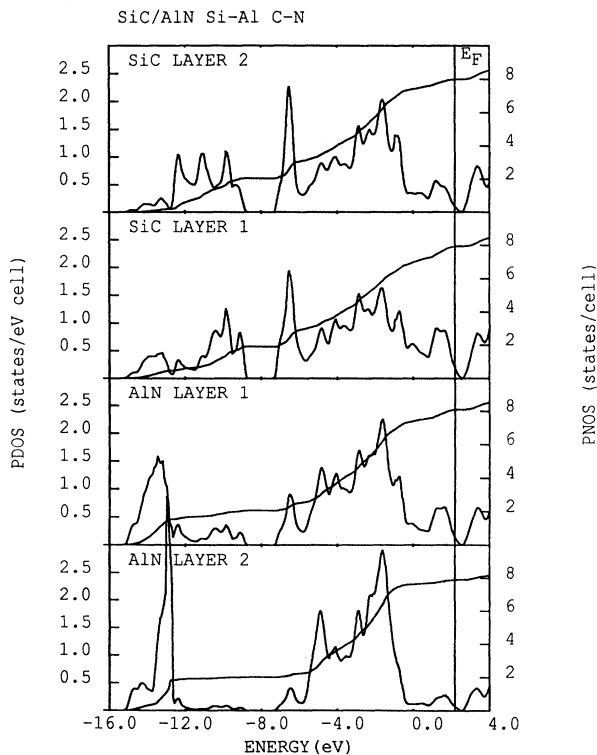


FIG. 3. Layer projected densities of states (PDOS) and their cumulative integral (PNOS) for SiC/AlN with Si-Al and C-N configuration.

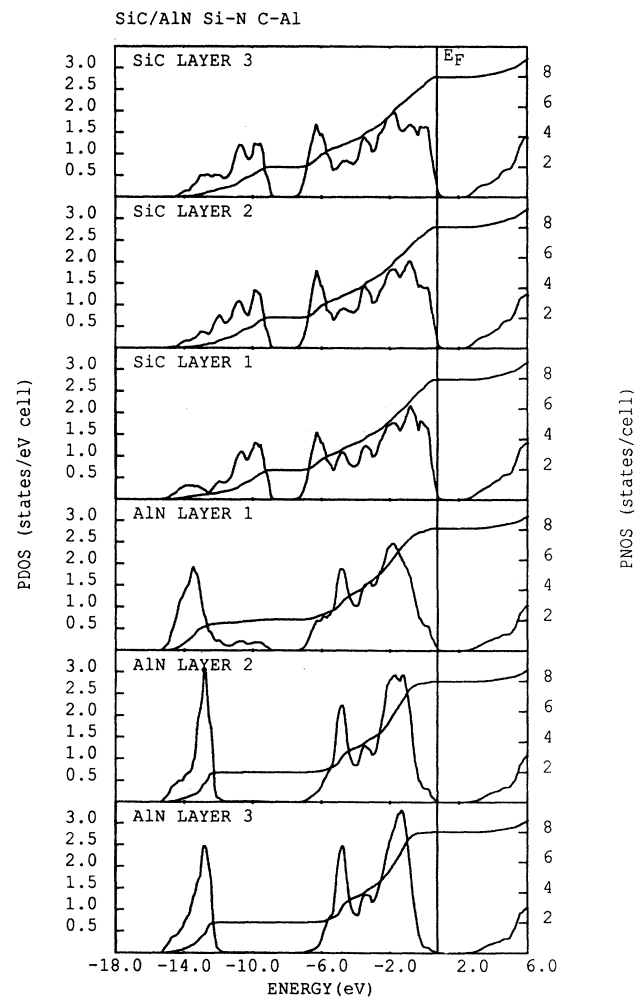


FIG. 4. Same as Fig. 3 for SiC/AlN with Si-N,C-Al configuration.

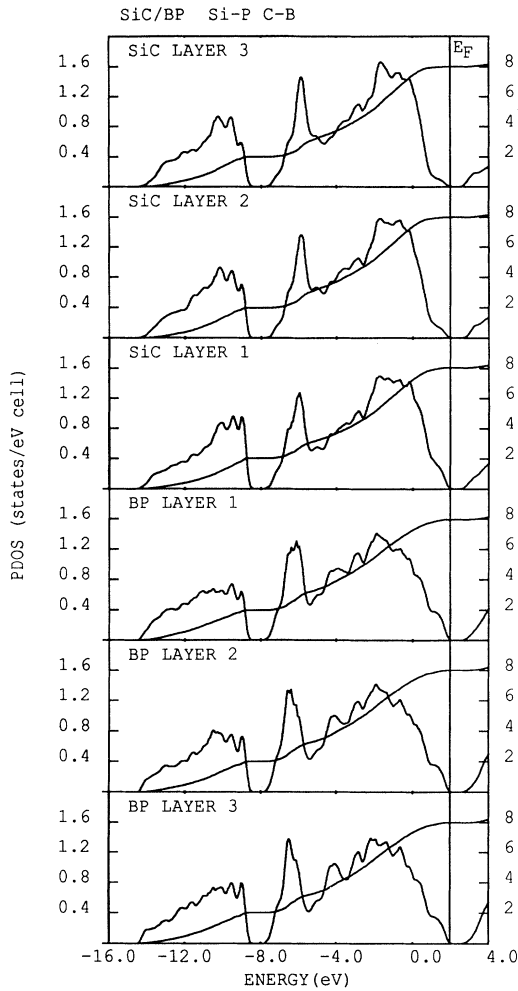


FIG. 5. Same as Fig. 3 for SiC/BP with Si-P,C-B configuration.

VI. CONCLUSIONS

In this paper, we have presented results for the bulk electronic structure and total-energy properties of cubic SiC, AlN, and BP and the (110) interfaces SiC/AlN and SiC/BP. In the Introduction, we have presented arguments why the (110) interface is supposed to be at least qualitatively representative of other interfaces as well.

We found that the interface energies of formation were similar for both systems. In the favorable bonding configuration, they are 0.45 and 0.50 eV/interface-unit-cell-area for SiC/AlN and SiC/BP, respectively. These are relatively small compared to our estimates of the surface energies (of the order of 2–3 eV). Consequently, the adhesion energies at these heterojunctions are only slightly weaker than the average surface energy of the corresponding individual semiconductors. These formation energies, however, are fairly large compared to a thermal energy at room temperature, and to corresponding results for other semiconductors such as AlAs/GaAs. They suggest

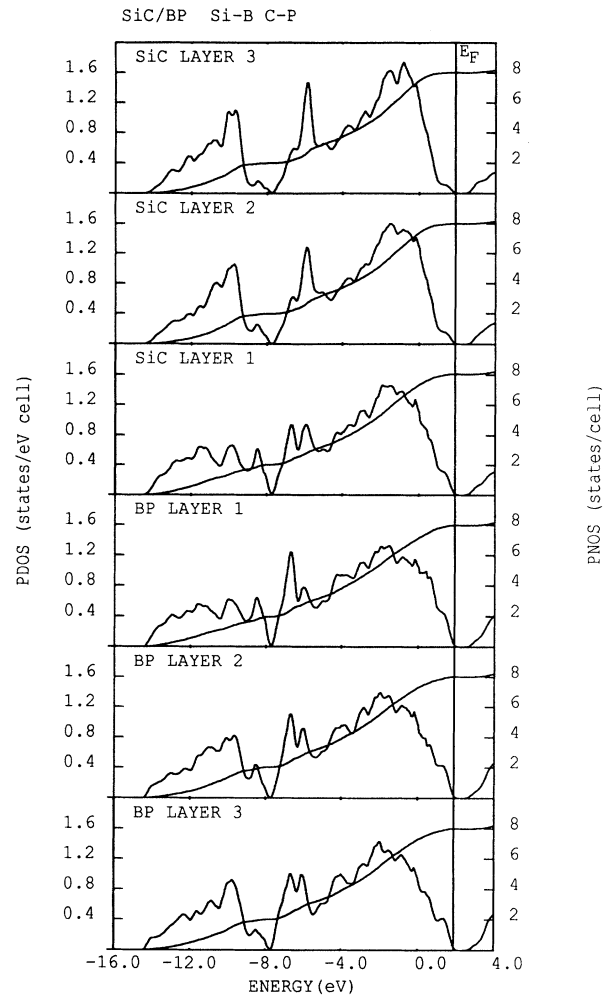


FIG. 6. Same as Fig. 3 for SiC/BP with Si-B,C-P configuration.

a fairly strong tendency towards disproportionation. Of course, this does not necessarily mean that disproportionation will occur rapidly or that heterostructures, superlattices or solid solutions of these semiconductors could not be formed. Barriers against diffusion could play a decisive role in these systems. We have presented a crude estimate of the maximum miscibility gap temperature of SiC-AlN solid solutions and found a value of 2500 ± 500 K in qualitative agreement with experiment.

The favorable bonding configurations were found to be Si—N,C—Al bonding and Si—B,C—P bonding, with the alternatives several eV higher in energy for the idealized geometry. As noted earlier, atomic relaxations would undoubtedly reduce the energy difference between the two configurations. Nevertheless, estimates of these effects that we made by utilizing comparisons to similar problems lead us to conclude that the alternative configurations would have energies of about an order-of-magnitude larger than the favorable ones even after relaxation of

local bond lengths are taken into account. The occurrence of the unfavorable bonding configurations can thus safely be ruled out. The main factor militating against the unfavorable bonding configurations is the larger electrostatic energy occurring when cations and anions have like ions as nearest neighbors. In other words, cations bond to anions across the interface. Whereas for SiC and AlN the ion characters are fairly obvious, it was found that BP has a seemingly anomalous ion character with B playing the role of anion. The origin of this anomaly is explained in terms of the deep-lying levels of B. The deep-lying levels of the other elements from the second row of the Periodic Table (C and N) lead to the rather high ionicities of SiC and AlN. In view of the unavoidable ambiguities related to the charge assignment to different atoms or ions in a solid, the ion character in BP was discussed in detail.

The bulk band gaps including an estimate of the *GW* correction to the LDA result were shown to be in fair agreement with experimental data for SiC and BP. For cubic AlN, where no data are available, we predict a band gap of ~ 5.1 eV. The band alignment was found to be of type I in the case of SiC/AlN, SiC having the higher valence-band maximum. For SiC/BP, the band alignment is found to be of type II with both materials having almost equal band gaps and BP having the higher valence-band maximum. The magnitudes and signs of the valence-band offsets and the magnitudes of the band gaps in these systems offer interesting opportunities for

electronic and electro-optical devices. In the case of BP which has a 4% larger lattice constant than SiC, our calculation showed that strain effects are smaller than 0.1 eV for the (110) interface. Energy differences of this order of magnitude are anticipated for different interface orientations or due to relaxation effects which were neglected here. Because of the lattice mismatch and associated strain, the results for the SiC/BP are still slightly preliminary in view of the problems of the ASA in dealing with distorted structures. We do not, however, expect, qualitative changes.

The local densities of states near the interface were presented and show characteristic interface localized features for the distinct bonding configurations, which may be helpful in confirming the interface bonding configurations when photoemission studies of these interfaces become available in the future.

ACKNOWLEDGMENTS

We thank O. Jepsen and M. van Schilfgaarde for making their LMTO programs available. This work was supported by the U.S. Defense Advanced Research Projects Agency (DARPA)—Office of Naval Research (ONR)—University Research Initiative (URI), Contract No. N00013-86-K-0773. Computing services from the Pittsburgh Supercomputing Center (PHY87-0036P) and Ohio Supercomputing Center (PDS-145) are acknowledged.

¹ *Diamond, Boron Nitride, Silicon Carbide and Related Wide Bandgap Semiconductors*, edited by J. T. Glass, R. Messier, and N. Fujimori, MRS Symposia Proceedings No. 162 (Materials Research Society, Pittsburgh, 1990).

² *Properties of II-VI Semiconductors: Bulk Crystals, Epitaxial Films, Quantum Well Structures, and Dilute Magnetic Systems*, edited by J. F. Schetzina, F. J. Bartoli, Jr., and H. F. Schaake, MRS Symposia Proceedings No. 161 (Materials Research Society, Pittsburgh, 1990).

³ W. A. Harrison, *Electronic Structure and Properties of Solids* (Freeman, San Francisco, 1980).

⁴ W. R. L. Lambrecht and B. Segall, *Phys. Rev. B* **40**, 9909 (1989).

⁵ D. W. Jenkins and J. D. Dow, *Phys. Rev. B* **39**, 3317 (1989).

⁶ S. Yugo and T. Kimura, *Phys. Status Solidi A* **59**, 363 (1980).

⁷ W. F. Knippenberg and G. Verspui, in *Silicon Carbide—1968*, edited by H. K. Henisch and R. Roy (Pergamon, New York, 1969), p. 51.

⁸ R. F. Rutz and J. J. Cuomo, in *Silicon Carbide—1973*, edited by R. C. Marshall, J. W. Faust, Jr., and C. E. Ryan (University of South Carolina Press, Columbia, 1974), p. 72.

⁹ M. J. Paisley, Z. Sitar, J. B. Posthill, and R. F. Davis, *J. Vac. Sci. Technol. A* **7**, 701 (1989); Z. Sitar, M. J. Paisley, B. Yan, J. Ruan, J. W. Choyke, and R. F. Davis, *ibid.* **B** **8**, 316 (1990).

¹⁰ G. A. Slack, *J. Phys. Chem. Solids* **34**, 321 (1973).

¹¹ G. A. Slack, R. A. Tanzilli, R. O. Pohl, and J. W. Vander-sande, *J. Phys. Chem. Solids* **48**, 641 (1987).

¹² W. A. Harrison, E. A. Kraut, J. R. Waldrop, and R. W. Grant, *Phys. Rev. B* **18**, 4402 (1978).

¹³ R. M. Martin, *J. Vac. Sci. Technol.* **17**, 178 (1980).

¹⁴ R. M. Wentzcovitch, M. L. Cohen, and P. K. Lam, *Phys. Rev. B* **36**, 6058 (1987); R. M. Wentzcovitch, K. J. Chang, and M. L. Cohen, *ibid.* **34**, 1071 (1986).

¹⁵ A. Zangvil and R. Ruh, *J. Am. Ceram. Soc.* **71**, 884 (1988), and references therein.

¹⁶ Sh. A. Nurmagomedov, A. N. Pikhtin, V. N. Razbegaev, G. K. Safaraliev, Yu. M. Tairov, and V. F. Tsvetkov, *Fiz. Tekh. Poluprovodn.* **23**, 162 (1989) [*Sov. Phys.—Semicond.* **23**, 100 (1989)].

¹⁷ W. R. L. Lambrecht and B. Segall in *Metal-Ceramic Interfaces*, Vol. 4 of *Acta-Scripta Metallurgica Proceedings Series*, edited by M. Rühle, A. G. Evans, M. F. Ashby, and J. P. Hirth (Pergamon, Oxford 1990), p. 29.

¹⁸ W. R. L. Lambrecht and B. Segall, in Ref. 1, p. 501.

¹⁹ W. R. L. Lambrecht and B. Segall, in *Interfaces in Metal-Matrix Composites, Part II. Mechanical Properties of Interfaces*, edited by R. Y. Lin, R. J. Arsenault, G. P. Martins, and S. G. Fishman (The Minerals, Metals and Materials Society, Warrendale, 1989), p. 319.

²⁰ W. R. L. Lambrecht, B. Segall, and O. K. Andersen, *Phys. Rev. B* **41**, 2813 (1990).

²¹ K. Nath and A. B. Anderson, *Phys. Rev. B* **40**, 7916 (1989).

²² A. Ourmazd, D. W. Taylor, J. Cunningham, and C. W. Tu, *Phys. Rev. Lett.* **62**, 933 (1989).

- ²³W. R. L. Lambrecht and B. Segall, *Phys. Rev. B* **41**, 2832 (1990).
- ²⁴P. Hohenberg and W. Kohn, *Phys. Rev.* **136**, B864 (1964); W. Kohn and L. J. Sham, *ibid.* **140**, A1133 (1965).
- ²⁵U. von Barth and L. Hedin, *J. Phys. C* **5**, 1629 (1972).
- ²⁶O. K. Andersen, *Phys. Rev. B* **12**, 3060 (1975); O. K. Andersen, O. Jepsen, and D. Glötzel, in *Highlights of Condensed-Matter Theory*, Proceedings of the International School of Physics "Enrico Fermi," Course LXXXIX, Varenna, 1983, edited by F. Bassani, F. Fumi, and M. P. Tosi (North-Holland, Amsterdam, 1985), p. 59; O. K. Andersen, O. Jepsen, and M. Šob, in *Electronic Band Structure and its Applications*, edited by M. Yussouff (Springer, Heidelberg, 1987).
- ²⁷D. Glötzel, B. Segall, and O. K. Andersen, *Solid State Commun.* **36**, 403 (1980).
- ²⁸G. B. Bachelet and N. E. Christensen, *Phys. Rev. B* **31**, 879 (1985).
- ²⁹N. E. Christensen, *Solid State Commun.* **68**, 959 (1988).
- ³⁰O. K. Andersen, M. Methfessel, C. O. Rodriguez, P. Blöchl, and H. M. Polatoglou, in *Atomistic Simulation of Materials: Beyond Pair Potentials*, edited by V. Vitek and D. J. Srolovitz (Plenum, New York, 1989), p.1.
- ³¹L. Brey, N. E. Christensen, and M. Cardona, *Phys. Rev. B* **36**, 2638 (1987).
- ³²P. Vinet, J. Ferrante, J. R. Smith, and J. H. Rose, *J. Phys. C* **19**, L467 (1986).
- ³³C. B. Duke and Y. R. Wang, *J. Vac. Sci. Technol. B* **4**, 1440 (1988).
- ³⁴G.-X. Qian, R. M. Martin, and D. J. Chadi, *Phys. Rev. B* **37**, 1203 (1988).
- ³⁵J. H. Rose, J. R. Smith and J. Ferrante, *Phys. Rev. B* **28**, 1835 (1983).
- ³⁶W. R. L. Lambrecht and B. Segall, *Phys. Rev. B* **41**, 2948 (1990).
- ³⁷Harrison's polarity essentially corresponds to the square root of the Phillips ionicity as defined in J. C. Phillips, *Bonds and Bands in Semiconductors* (Academic, New York, 1973).
- ³⁸H. H. Woodbury and G. W. Ludwig, *Phys. Rev.* **124**, 1083 (1961).
- ³⁹Although A. G. Zubatov, I. M. Zaritskil, S. N. Lukin, E. N. Mokhov, and V. G. Stepanov, *Fiz. Tverd. Tela* (Leningrad) **27**, 322 (1985) [*Sov. Phys.—Solid State* **27**, 197 (1985)] have found B to substitute on the Si site, C. Wang, J. Bernholc, and R. F. Davis, in Ref. 1, p. 475, have argued that this could be due to a C-rich nonstoichiometric SiC.
- ⁴⁰See, e.g., Harrison, Ref. 3, p. 20 and following, for a discussion of ionicity and covalency in heteropolar bonds.
- ⁴¹D. M. Bylander and L. Kleinman, *Phys. Rev. Lett.* **59**, 2091 (1987).
- ⁴²A. A. Mbaye, L. G. Ferreira, and A. Zunger, *Phys. Rev. Lett.* **58**, 49 (1987).
- ⁴³A. Sher, M. van Schilfgaarde, A.-B. Chen, and W. Chen, *Phys. Rev. B* **36**, 4279 (1987).
- ⁴⁴J. W. D. Connolly and A. R. Williams, *Phys. Rev. B* **27**, 5169 (1983).
- ⁴⁵R. Kikuchi, *Phys. Rev.* **81**, 988 (1951).
- ⁴⁶D. de Fontaine, in *Solid State Physics, Advances in Research and Applications*, edited by F. Seitz, D. Turnbull, and H. Ehrenreich (Academic, New York, 1979), Vol. 34, p. 73.
- ⁴⁷See C. Kittel and H. Kroemer, *Thermal Physics*, 2nd ed. (Freeman, San Francisco, 1980), Chap. 11 for a similar treatment of the binary alloy problem.
- ⁴⁸A. Zunger, L. G. Ferreira, and S.-H. Wei, in *Atomic Scale Calculations in Materials Science*, edited by J. Tersoff, D. Vanderbilt and V. Vitek, MRS Symposia Proceedings No. 141 (Materials Research Society, Pittsburgh, 1989), p. 177.
- ⁴⁹C. Cheng, R. J. Needs, and V. Heine, *J. Phys. C* **21**, 1049 (1988).
- ⁵⁰W. R. L. Lambrecht (unpublished).
- ⁵¹P. J. H. Denteneer, in Ref. 48, p. 343.
- ⁵²K. J. Chang and M. L. Cohen, *Solid State Commun.* **50**, 487 (1984).
- ⁵³C.-O. Almbladh and U. von Barth, *Phys. Rev. B* **31**, 3231 (1985).
- ⁵⁴L. J. Sham and W. Kohn, *Phys. Rev.* **145**, 561 (1966).
- ⁵⁵J. P. Perdew and M. Levy, *Phys. Rev. Lett.* **51**, 1884 (1983).
- ⁵⁶L. J. Sham and M. Schlüter, *Phys. Rev. Lett.* **51**, 1888 (1983).
- ⁵⁷O. Gunnarsson and K. Schönhammer, *Phys. Rev. Lett.* **56**, 1968 (1986); K. Schönhammer and O. Gunnarsson, *J. Phys. C* **20**, 3675 (1987).
- ⁵⁸R. W. Godby, M. Schlüter, and L. J. Sham, *Phys. Rev. Lett.* **56**, 2415 (1986); *Phys. Rev. B* **37**, 10159 (1988).
- ⁵⁹W. R. L. Lambrecht and B. Segall, *Phys. Rev. B* **40**, 7793 (1989).
- ⁶⁰L. Hedin, *Phys. Rev.* **139**, A796 (1965); L. Hedin and S. Lundqvist, in *Solid State Physics, Advances in Research and Applications*, edited by F. Seitz, D. Turnbull, and H. Ehrenreich (Academic, New York 1969), Vol. 23, p. 1.
- ⁶¹M. S. Hybertsen and S. G. Louie, *Phys. Rev. Lett.* **55**, 1418 (1985); *Phys. Rev. B* **34**, 5390 (1986).
- ⁶²W. Hanke and L. J. Sham, *Phys. Rev. B* **38**, 13361 (1988).
- ⁶³F. Bechstedt and R. Del Sole, *Phys. Rev. B* **38**, 7710 (1988).
- ⁶⁴*Numerical Data and Functional Relationships in Science and Technology*, edited by O. Madelung, Landolt-Börnstein, New Series, Group III, Vol. 17a (Springer, Berlin, 1982).
- ⁶⁵M. Cardona and N. E. Christensen, *Phys. Rev. B* **35**, 6182 (1987).
- ⁶⁶C. G. Van de Walle and R. M. Martin, *Phys. Rev. Lett.* **62**, 2028 (1989).
- ⁶⁷C. G. Van de Walle and R. M. Martin, *Phys. Rev. B* **34**, 5621 (1986).
- ⁶⁸D. D. Wagman, W. H. Evans, V. B. Parker, I. Halow, S. M. Baily, and R. H. Shumm, *Selected Values of Chemical Thermodynamics Properties, Tables for the First Thirty-Four Elements in the Standard Order of Arrangement*, Natl. Bur. Stand. (U.S.) Circ. No. 270-3 (U.S. GPO, Washington, D.C., 1968).
- ⁶⁹W. Wetzling and J. Windscheif, *Solid State Commun.* **50**, 33 (1984).